Vanishing Magnetic Shear And Electron Transport Barriers In The RFX-Mod Reversed Field Pinch

M. Gobbin, D. Bonfiglio, D. F. Escande, A. Fassina, L. Marrelli, A. Alfier, E. Martines, B. Momo, and D. Terranova

Consorzio RFX, Associazione EURATOM-ENEA sulla Fusione Corso Stati Uniti, 4 35127 Padova-Italy

(Received 19 August 2010; published 13 January 2011)

We define the safety factor q for the helical plasmas of the experiment RFX-mod by accounting for the actual three-dimensional nature of the magnetic flux surfaces. Such a profile is not monotonic but goes through a maximum located in the vicinity of the electron transport barriers measured by a high resolution Thomson scattering diagnostic. Helical states with a single axis obtained in viscoresistive magnetohydrodynamic numerical simulations exhibit similar nonmonotonic q profiles provided that the final states are preceded by a magnetic island phase, like in the experiment.

DOI: 10.1103/PhysRevLett.106.025001 PACS numbers: 52.55.Lf, 52.25.Xz, 52.55.Dy

Internal transport barriers (ITBs) occurring spontaneously in magnetized plasmas with high input power are zones where transport is strongly reduced and may come close to neoclassical expectations. Therefore understanding such barriers is a critical outstanding issue in magnetic fusion science. In particular, ITB triggering mechanisms, such as the reversal of magnetic shear and the role of three-dimensional field shaping [1], are intensively investigated both in Tokamaks and Stellarators [2–5]: the improved confinement associated to such plasmas is, indeed, considered to be relevant for steady state reactors. The investigation of the ITB formation process recently got a new clue when electron ITBs were found to exist in the RFX-mod reversed field pinch experiment ($R = 2m$, $a = 0.459m$) [6]. During most of the duration of the flat top of RFX-mod high current discharges (up to 1.7 MA [7]), the plasma self-organizes into a helical state characterized by magnetic surfaces nested around a single helical axis, enclosed in an almost axisymmetric boundary. This state is the result of two successive bifurcations occurring when the current is progressively increased. The first one makes the plasma leave the multiple helicity state, characterized by the presence of several resonant modes with similar amplitudes, and reach the quasisingle helicity state which displays a single dominant mode and secondary ones with smaller amplitudes. For intermediate currents, in a first quasisingle helicity stage, the magnetic topology includes a magnetic island. Therefore the magnetic field displays two magnetic axes: the unperturbed axisymmetric one and the one related to the island O point. For such states, termed double axis (DAx), a magnetic island with electron ITB [8] winds around the magnetic axis [9] and is characterized by a maximum of the electron temperature tightly correlated to the location of the O point as reconstructed by external measurements. The second bifurcation changes the topology of the magnetic field through the coalescence of the axisymmetric O point with the island X point. The former island O point becomes the only magnetic axis, which motivates the term single helical axis (SHAx) for this kind of quasisingle helicity state [10]. Such transition (the two stages) finds a straight similarity with the dynamics described in 3D viscoresistive nonlinear MHD [11,12]. In SHAx states, the region inside the ITB [13] spans a significantly bigger volume than in DAx states, with similar maximum electron temperature gradients at the barrier. Plasma properties such as electron temperature, soft x rays emissivity, and electron density have been found to be constant on helical magnetic surfaces [14] reconstructed with independent measurements, indicating that SHAx states are described by a MHD equilibrium characterized by almost invariant magnetic surfaces, in contrast with the low current multiple helicity states.

This Letter shows that the ITBs are associated with a flattening or a reversal of the magnetic shear profile of the quasisingle helicity equilibria. This has been estimated by computing, for the first time in reversed field pinch physics, the profile of the safety factor q of the helical magnetic surfaces. Numerical simulations with the MHD SPECYL code [12] show that q profiles similar to the experimental ones are observed for SHAx states developing from a DAx state. The location of the electron transport barrier in both DAx and SHAx states, as measured by the Thomson scattering diagnostic, is found to be well correlated with the region where the experimental estimate of q features a null shear point.

The first part of this Letter provides the calculation of the q profiles for the SHAx and DAx states, and compares them with the standard axisymmetric ones. The correlation between the location of the maximum of the q profile and the location of the ITB is then characterized statistically. Although helical RFX-mod plasmas differ in many aspects from those in other magnetic configurations, the results described in this Letter share some general characteristics and implications with the electron internal transport barrier in Tokamaks and Stellarators too, as will be discussed at the end of the Letter.

In the reversed field pinch, the safety factor profile of the axisymmetric configuration monotonically decreases from

the plasma center ($q_{\rm axi} \sim 0.15$ in RFX-mod) to the edge ($q_{\rm axi} \sim -0.02$) and is always well below unity. As a consequence, many internal resistive-kink-tearing modes with poloidal number $m = 1$ and toroidal number $n > 3R/2a$ are resonant in RFX-mod. In RFX-mod the dominant mode in quasisingle helicity states (both DAx and SHAx) is the $m = 1$ and $n = -7$ one, i.e., the innermost resonant mode. The reconstruction of the helical magnetic field is obtained by combining a Shafranov axisymmetric equilibrium, assuming circular flux surfaces, and a Newcomb calculation of the perturbed poloidal and toroidal magnetic fluxes [15,16] using the measured magnetic field at the edge and the plasma current, as described in [17]. The agreement between the shape of the corresponding magnetic surfaces and the isoemissivity surfaces of X tomography gives confidence in this reconstruction [18]. Magnetic field lines are then integrated by means of the ORBIT code [19]. Figure 1(a) for a SHAx state and Fig. 1(d) for a DAx state display Poincaré plots of the magnetic field lines exhibiting the deformation due to the dominant quasisingle helicity mode. The magnetic field structure in a SHAx state is composed by nested helical magnetic surfaces, the innermost one being the helical axis. For every surface we

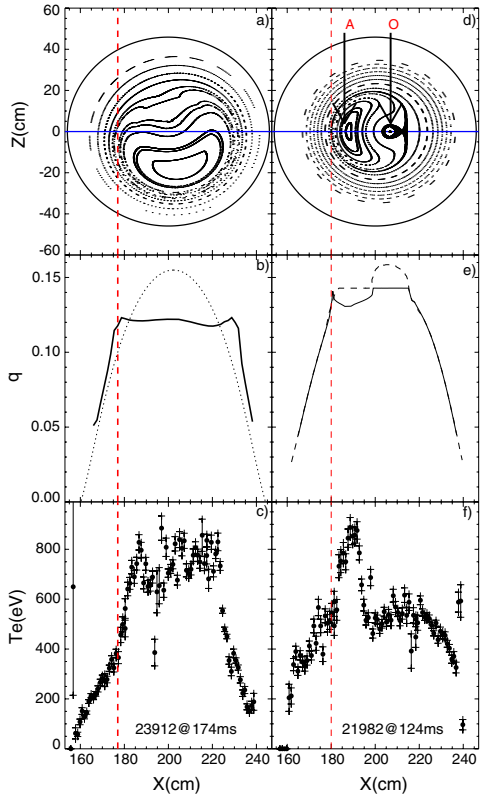

FIG. 1 (color online). (a),(d) Poincaré plot for a SHAx and DAx case, respectively. (b) Safety factor profile for a SHAx state (continuous) and $q_{\rm axi}$ (e) q for DAx case. Continuous (respectively, dashed) line represents the q computed with respect to the O point **O**; (respectively, former axisymmetric axis A). (c), (f) Thomson scattering profile for a SHAx and a DAx case, respectively, measured along the diameter shown with a horizontal line in (a) and (d).

numerically computed the inverse of the safety factor, i.e., the rotational transform ι, defined as the average of the total poloidal angle around the helical axis after one toroidal transit [20]:

$$\iota = \frac{1}{2\pi} \lim_{n\to\infty} \frac{\sum_{k=1}^{n} \iota_k}{n} \tag{1}$$

where ι_k represents the rotation of poloidal angle ($\Delta\theta_k$) around the helical axis resulting from the kth toroidal transit.

For the SHAx case shown in Fig. 1(a) we have numerically computed $q = 1/\iota$ by applying Eq. (1): the profile, along the magnetic surfaces intersection with a diameter, is shown in Fig. 1(b). By defining a set of flux coordinates, following the algorithm described in [14,21], it is possible to cast the magnetic field representation in Hamiltonian form. Thus, the rotational transform for each helical flux surface is computed in a set of straight field lines coordinates obtained by performing a canonical transformation to action angle coordinates. The q profile in SHAx cases obtained with this analytical method coincides with the one computed numerically using Eq. (1) and reported in Fig. 1(b). For reference, the axisymmetric $q_{\rm axi}$ profile, obtained considering the axisymmetric equilibrium fields only, is also shown in the figure (dotted curve). We observe that while the $1/7$ resonant surface exists in the axisymmetric $q_{\rm axi}$ profile, the q values for the helical surfaces are always lower than $1/7$; equivalently, ι is always above 7.

The q profile in SHAx states exhibits a maximum and its slope changes sign, implying the presence of a significant magnetic shear. Correspondingly, the steep electron transport gradient occurs very near this region, as shown in Fig. 1(c) where a Thomson scattering temperature profile along a diameter (horizontal line) is shown. The presence of a maximum in the q profile is a typical feature of a mode whose helicity is resonant in the axisymmetric equilibrium, i.e., when the final SHAx state is the result of a transition from a DAx state. This has been observed in viscoresistive nonlinear MHD numerical simulations of SHAx equilibria, performed in cylindrical geometry with the SPECYL code [12]. The geometry of the SPECYL simulations and their initial conditions are such that the innermost resonant mode is the $n = -10$. The q profile of the nonlinearly saturated helical state is obtained by computing for each helical magnetic surface both the poloidal and toroidal flux functions and by applying the standard definition $d\psi_{\rm tor}(\rho)/d\psi_{\rm pol}(\rho)$ where ρ is a normalized flux surface label. It is interesting to note that the shape of the q profile depends on the n number of the mode [see Fig. 2]. In particular the $n = -8$ and $n = -9$ SHAx equilibria, which are obtained after the saturation of a nonresonant kink mode (without going through a DAx state), are characterized by a monotonic q profile. On the other hand, when the SHAx equilibrium is reached as a saturation of a resonant resistive kink-tearing mode (as for -10 and for -11 helicities), i.e., after a transition from a DAx to a

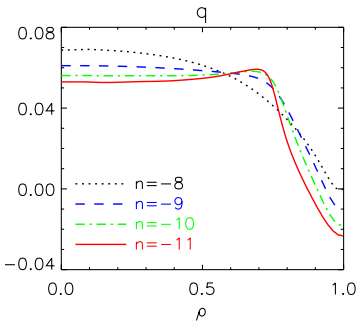

FIG. 2 (color online). q profiles corresponding to different helical equilibria provided by viscoresistive MHD simulations (SPECYL code) for $m = 1$ modes with n varying from $n = -11$ to $n = -8$.

SHAx topology, the corresponding q profile takes a peaked shape. These numerical findings agree with q estimates in experimental SHAx states since they develop from a DAx topology [22].

The concept of q is useful in analyzing DAx states, where the separatrix splits the plasma in three regions, as shown in Fig. 1(d) with the locations of the original magnetic axis and of the island O point clearly visible. In such states, in fact, electron temperature gradients build up, and the foot of the gradient is close to the separatrix, where a change of a properly defined q profile occurs. For each surface, the definition (1) can be applied with respect to either the axisymmetric axis or the magnetic island O point. The q for surfaces outside the separatrix do not depend on the choice of the axis, as they contain both of them. The same does not apply to the two classes of surfaces inside the separatrix, i.e., the surfaces around the axis and the ones inside the magnetic island. In both cases, the estimate of the rotational transform around an axis outside the surface gives a degenerate result: every surface of the magnetic island winds 7 times around the magnetic axis [point A in Fig. 1(d)], and each core surface winds the same number of times around the magnetic island O point [point O in Fig. 1(d)]. Every surface is characterized by a different value of q if an axis internal to it is considered: q is less than $1/7$ inside the magnetic island, while it is greater than $1/7$, for the other surfaces. Indeed the separatrix is the attractor of the X point, which is a remnant of the axisymmetric resonant surface whose q_{axi} was exactly $1/7$.

The experimental relation between the positions of the electron temperature gradient foot and the shear reversal of q in both DAX and SHAx states, have been investigated statistically. A set of 55 Thomson scattering profiles of similar plasmas have been considered. The discharges had plasma currents in the range $1 < I_p < 1.6$ MA and electron density: $2 \times 10^{19} < n_e < 4 \times 10^{19}$ m^{-3}. The parameters $F = B_\phi/\bar{B}_\phi$ and $\Theta = B_\theta/\bar{B}_\phi$, with $B_\phi(a)$ the toroidal field at the edge and $\bar{B}_\phi$ its average over the plasma volume are, respectively, in the range $-0.11 < F < -0.016$ and $1.36 < \Theta < 1.46$. The dominant perturbation $(1, -7)$ has a toroidal component at the edge of the plasma in the range $5\ \mathrm{mT} < b^{1,7}_\phi(a) < 25\ \mathrm{mT}$ corresponding to 1%–5% of total field at $r = a$. The location of the ITB has been determined by the intersection of straight lines fitting the Thomson scattering profiles in separate regions. The uncertainty in the intersection determinations is estimated by propagating the error in the linear fits. For each temperature profile, the equilibrium and the magnetic perturbation have been computed based on experimental data and the q profile has been derived by the rotational transform technique. The error bars on the location of the maximum of q are estimated by considering for each data point the helical equilibrium reconstructed with slightly different assumptions on the internal axisymmetric profiles. Electron temperature gradients are observed in both sides along the diameter, but to reduce the uncertainty, for the statistical analysis we have chosen the steepest one: this corresponds to regions with a greater change of the slope for the q profile.

The resulting relation between the foot of the gradient of T_e and the location of the maximum of q is shown in Fig. 3. It can be clearly seen that in both the DAx and SHAx cases the two locations are well correlated and coincide within a few centimeters. For the DAx case the steep gradient is systematically beginning slightly inside the separatrix, while for the SHAx case this gradient may be on any side of the maximum q surface up to experimental errors. This may be due to the fact that in the SHAx case the separatrix expulsion reduces the level of the magnetic chaos [11].

Another important point concerns the width of the region of slightly reversed shear: it is found that it increases as long as the amplitude of the helical magnetic field grows. This has been numerically investigated by considering a typical RFX-mod discharge with $I_p = 1.1$ MA and $F = -0.03$; the amplitude of the dominant $m = 1$, $n = -7$ mode has been artificially increased from a value of $b^{\phi}_{1,7}(a)/B(a) = 0.02\%$ to a maximum of 10%. The corresponding profiles of the safety factor have been computed as described in the previous sections. Results are reported in Fig. 4: the maximum value reached by q

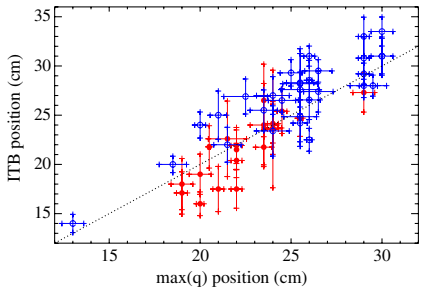

FIG. 3 (color online). Position of the ITB vs the q maximum location for RFX-mod experimental DAx (full points) and SHAx states (empty points). Error bars in the abscissas are due to uncertainties in equilibrium reconstruction.

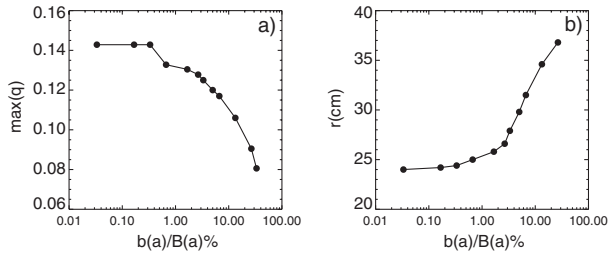

FIG. 4. (a) Maximum of q as function of the dominant mode amplitude at the edge of the plasma normalized to the equilibrium field; (b) q maximum position on the y axis.

(panel a) and the radial position r of the q maximum (panel b) have been plotted versus the perturbation amplitude. In a DAx state a stronger helical field only increases the radial extent of the magnetic island and keeps the q value at the separatrix equal to $1/7$. When the helical perturbation is high enough to induce the bifurcation to the SHAx state, i.e., when the maximum q radius becomes comparable to the resonant radius of the axisymmetric configuration, the weak shear volume increases and the maximum q value decreases. Even though the radial position of the ITB also depends on the plasma current and the reversal parameter F (that for this particular numerical scan were held fixed), these results suggest that an increased amplitude of the helical field, which can be expected since at higher plasma currents we are getting closer to the helical equilibrium state, might lead to wider helical regions of enhanced electron temperature. This issue suggests that it may be possible to control the ITB location and its extent by suitably modifying the edge boundary conditions, by exploiting the network of active feedback coils of RFX-mod.

The results shown in this Letter share some features with electron internal transport barrier (eITB) observed in other configurations. As far as Tokamaks are concerned, during negative shear discharges the radius of the eITB is found in several experiments to be correlated with the location of $q_{\min}$ [3]. The null point in the q shear of RFX-mod helical plasmas could act to separate the resonances associated with residual magnetic modes as also discussed in [23], reducing the transport due to magnetic chaos. This may be related to the observed partially stochastic domain surrounding magnetic islands in DAx states [24]. Electron transport barriers in Tokamaks may also occur together with the ion ITBs: the latter are characterized by a flow shear which further suppresses the turbulence in the barrier region [3]. It is unclear, at present, whether an ion transport barrier is also present in RFX-mod SHAx states as it may occur in Tokamaks: passive spectroscopy measurements indicate that $T_i/T_e = 0.7$ for ion species located near the barrier but no information on the T_i spatial profile is currently available [7]. On the other hand, RFX-mod eITB occur when the core topology is helical, similarly to improved confinement regimes (core electron-root confinement [25]) in Stellarator devices. It has been reported [26,27] that ITBs in helical devices are associated to a strong radial electric field. Such a field is positive inside the barrier (electron root) and negative outside (ion root), and it is determined by the ambipolarity condition, predicted by neoclassical transport theory in low-collisionality helical plasmas. The E_r shear layer produced in this way would act to stabilize the turbulent component of transport [28]. Therefore similar transport reduction mechanisms may be at work, even though details may differ: in fact, both chaos reduction and flow shear may play an important role in the formation of RFX-mod eITBs.

We would like to thank S. Cappello and M. E. Puiatti for helping us in improving the manuscript. This work was supported by the European Communities under the contract of Association between EURATOM/ENEA. The views and opinions expressed herein do not necessarily reflect those of the European Commission.

[1] A. H. Boozer, Phys. Plasmas **5**, 1647 (1998).
[2] K. Lackner, Plasma Phys. Controlled Fusion **42**, B37 (2000).
[3] J. W. Connor *et al.*, Nucl. Fusion **44**, R1 (2004).
[4] X. Garbet and R. E. Waltz, Phys. Plasmas **3**, 1898 (1996).
[5] K. Ida *et al.*, Phys. Rev. Lett. **91**, 085003 (2003).
[6] P. Sonato *et al.*, Fusion Eng. Des. **66-68**, 161 (2003).
[7] M. E. Puiatti *et al.*, Plasma Phys. Controlled Fusion **51**, 124031 (2009).
[8] A. Alfier *et al.*, Plasma Phys. Controlled Fusion **50**, 035013 (2008).
[9] P. Franz *et al.*, Phys. Plasmas **13**, 012510 (2006).
[10] R. Lorenzini *et al.*, Phys. Rev. Lett. **101**, 025005 (2008).
[11] D. F. Escande *et al.*, Phys. Rev. Lett. **85**, 3169 (2000).
[12] S. Cappello, Plasma Phys. Controlled Fusion **46**, B313 (2004).
[13] M. Valisa *et al.*, Plasma Phys. Controlled Fusion **50**, 124031 (2008).
[14] R. Lorenzini *et al.*, Nature Phys. **5**, 570 (2009).
[15] W. A. Newcomb, Ann. Phys. (Leipzig) **10**, 232 (1960).
[16] P. Zanca and D. Terranova, Plasma Phys. Controlled Fusion **46**, 1115 (2004).
[17] I. Predebon *et al.*, Phys. Rev. Lett. **93**, 145001 (2004).
[18] F. Bonomo *et al.*, Nucl. Fusion **49**, 045011 (2009).
[19] R. B. White and M. S. Chance, Phys. Fluids **27**, 2455 (1984).
[20] W. D. D'Haeseleer *et al.*, *Flux Coordinates and Magnetic Field Structure* (Springer-Verlag, Berlin, 1991).
[21] B. Momo *et al.*, in *Proceedings of the 37th EPS Conference on Plasma Physics*, 34A, P4.147 (EPS, Dublin, 2010).
[22] R. Lorenzini *et al.*, Phys. Plasmas **16**, 056109 (2009).
[23] T. Tala and X. Garbet, C.R. Physique **7**, 622 (2006).
[24] M. Gobbin *et al.*, Plasma Phys. Controlled Fusion **51**, 065010 (2009).
[25] M. Yokoyama *et al.*, Nucl. Fusion **47**, 1213 (2007).
[26] F. Castejon *et al.*, Nucl. Fusion **42**, 271 (2002).
[27] J. Lore *et al.*, Phys. Plasmas **17**, 056101 (2010).
[28] F. Wagner *et al.*, Plasma Phys. Controlled Fusion **48**, A217 (2006).